

A distributed algorithm for UAV-based communication networks using constrained extremum seeking

Chwen-Kai Liao*, Chris Manzie*, Airlie Chapman**

* *Department of Electrical and Electronic Engineering*
(*chwenkail@student.unimelb.edu.au; manziec@unimelb.edu.au*)

** *Department of Mechanical Engineering (e-mail:*
airlie.chapman@unimelb.edu.au)

Melbourne Information, Decision & Autonomous Systems Lab
The University of Melbourne, Parkville, VIC 3010, Australia

Abstract: Unmanned autonomous vehicles offer a solution to maintaining adaptive multi-hop communication paths when fixed infrastructure is not available, as may be the case in disaster recovery or in contested environments. Some of the potential challenges these networks face are changing environmental conditions, changing numbers of available agents and the need to avoid certain domains. In this paper, a distributed implementation of a constrained extremum seeking approach is proposed to optimise the signal power along the communication chain by adapting vehicle locations within allowable regions. The approach is demonstrated via simulations that consider both homogeneous and heterogeneous signal transmission pathways.

Keywords: Extremum seeking, constrained optimisation, mobile ad hoc network

1. INTRODUCTION

With the growing prevalence of wireless sensor network technologies and Internet of Things, mobile ad-hoc networks are an important enabler to provide reliable communication services (Rawat et al., 2014). In infrastructure-scarce scenarios such as might be encountered in disaster relief, a mobile ad-hoc network that can self-configure by changing the positions of agents, and/or accommodate the addition or removal of agents to provide solid multihop communications over a wireless communication channel, is an important tool.

In this paper, we consider the network to consist of a team of quadrotor-mounted wireless communication relays. In general, the wireless communication quality of two nodes in the network strongly depends on the distance between them; however, spatial- or time-varying environmental factors like humidity, fading coefficient and the transmitter's battery capacity can lead to an inaccurate estimation of the signal power distribution for each node. This can lead to a suboptimal deployment if the imprecise signal model is used. Furthermore, it may be undesirable to permanently locate agents above certain landforms such as forests and lakes which impact safe vehicle retrieval, or above other non-flight areas (e.g. helicopter landing zones or areas where adversaries are detected). To address this type of problem, we seek a model-free approach to optimise online the weakest signal power link within the network (i.e. the transmission bottleneck) by dynamically positioning the quadrotor-mounted communication relays, whilst also restricting the quadrotors from within designated no-

go areas. To solve this area-constrained wireless signal chaining problem, a recently proposed output constrained extremum seeking controller (ESC) (Liao et al., 2019) is adapted to provide a distributed implementation across a fleet of vehicles.

There are three main contributions of this work relative to similar schemes proposed previously in the literature:

- Other than Dixon and Frew (2009) which only considers optimising the throughput of the wireless communication chain, the strategy we propose also takes into account the both known and detected area constraints as well as disturbances;
- Different from Zhang et al. (2007) and Dürr et al. (2011) that inject perturbation signals to actuators of the vehicle, we proposed an inner-outer loop constrained extremum seeking scheme which explicitly takes into account the internal vehicle stabilising and tracking controller so that the proposed framework is applicable to more general vehicle dynamics;
- Unlike Min et al. (2016); Hasan et al. (2017) which utilise a distance or channel quality model to solve the optimum locations for deploying signal relay nodes, the proposed scheme is non-model based. This removes the reliance encountered by model-based design approaches when the environment and the signal model are highly uncertain.

The paper is laid out as follows. In the following section the nomenclature used throughout is defined. The proposed distributed approach is then outlined and the assumptions required for the theoretical guarantees of (Liao et al., 2019) are tested. Finally, simulation results are presented that validate the proposed approach with homogeneous and

* C Manzie and A Chapman acknowledge the support of the DCRC on Trusted Autonomous Systems.

heterogeneous agents acting under positional constraints indicative of a no-fly region.

2. NOMENCLATURE

A bold lower-case letter stands for a vector, e.g. \mathbf{a} , and a matrix is represented as a bold upper-case letter, e.g. \mathbf{A} . The block diagonal matrix formed by m number of \mathbf{A} matrices on its diagonal entries is $\text{diag}(\mathbf{A})_m$. The l_2 norm of a vector is $\|\cdot\|$. A non-empty set, \mathcal{A} , has a boundary denoted by $\partial\mathcal{A}$.

The function $\beta(\cdot, \cdot)$ is class \mathcal{KL} if $\beta(\cdot, \cdot) : \mathbb{R}_{\geq 0} \times \mathbb{R}_{\geq 0} \rightarrow \mathbb{R}_{\geq 0}$ is non-decreasing in its first argument, strictly decreasing in the second argument. Without loss of generality, $\beta(0, t) = 0 \forall t \geq 0$.

The finite graph \mathcal{G} is defined as a pair $\mathcal{G}(V, E)$, where V and E are the sets of vertices and edges. $ij \in E$ is the existing edge between v_i and v_j in $\mathcal{G}(V, E)$.

The following smooth approximations of *minimum*, *saturation* and *switching* functions that preserve differentiability and respectively denoted as $\Psi(\cdot)$, $\Omega(\cdot, \cdot)$ and $\sigma(\cdot)$ are used for $x \in \mathbb{R}$; $\mathbf{a} \in \mathbb{R}^n$ with $c_1 = 10$; $c_2 = 10^3$:

$$\Psi\{a_1, \dots, a_n\} := \frac{\sum_{k=1}^n a_k \cdot \exp(-c_1 a_k)}{\sum_{k=1}^n \exp(-c_1 a_k)} \quad (1)$$

$$\Omega(x) := \frac{2}{1 + \exp(-x)} - 1 \quad (2)$$

$$\sigma(x) := \frac{1}{1 + \exp(-c_2 x)} \quad (3)$$

3. PROBLEM FORMULATION

3.1 Proposed approach

We consider the scenario that there are $n + 2$ nodes in the chained wireless data-link, where each node has a label $i = 0, 1, \dots, n + 1$. In addition, we set node $i = 0$ and $i = n + 1$ as fixed end nodes representing two base stations, while nodes $i = 1, \dots, n$ are quadrotor-mounted wireless communication relays that can navigate in the space. The communication topology considered herein is a simple path graph as shown in Fig. 1. Under this communication topology, the quadrotor-mounted node (agent) i communicates with nodes (agents) $i - 1$ and $i + 1$ only.



Fig. 1. The considered graph communication topology, denoted $\mathcal{G}(V, E)$.

During this communication, each agent is assumed to be able to measure the respective signal strength from each of its neighbours. No *a priori* knowledge of the signal power functions of individual agents is assumed to exist. The implication of this assumption is that a non-model-based approach to the problem must be employed, leading to the self assembly of agents towards preferable locations to maximise the communication throughput. Furthermore, it is desirable that the algorithm for agent localisation

is distributed, so that no centralised communication is required. Thus within each agent, a hierarchical control structure is proposed that consists of an outer loop that sets a reference position, $\mathbf{u}_i := [x_i^g, y_i^g, z_i^g]^T$ in (x, y, z) -coordinates, and an inner loop that utilises the position error between guidance coordinates and the current position of vehicle, $\mathbf{x}_i := [x_i, y_i, z_i]^T$, to command the motors.

Given the desire to not consider certain specified no-fly zones, it is apparent that a constrained, non-model based online optimisation approach is a potential outer-loop strategy that can readily be implemented in a distributed fashion. The proposed structure is illustrated in Fig 2, and based on (Liao et al., 2019).

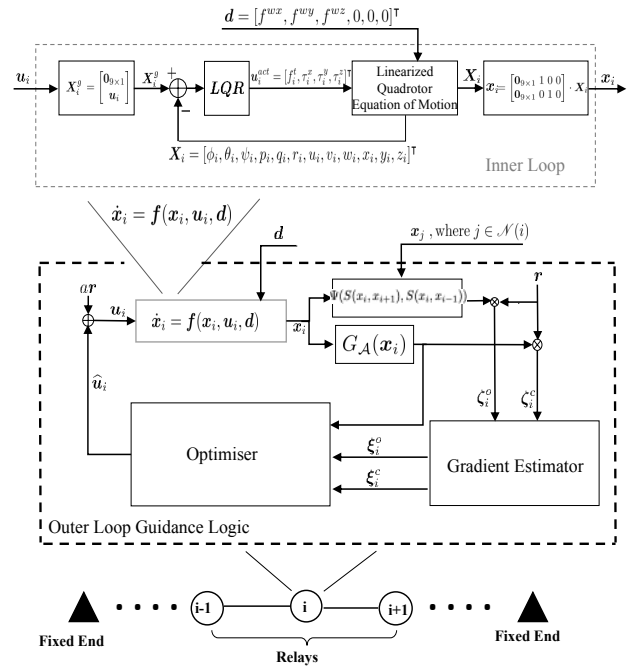


Fig. 2. The proposed hierarchical strategy. The outer-loop is an output constrained ESC. For relay node i , the objective function Q_i corresponds to the data-link power to be maximized; whilst $G_{\mathcal{A}}$ is the operation area constraint.

In the following subsections, the Assumptions that underpin the constrained extremum seeking approach of (Liao et al., 2019) will be shown to hold, and thus the semi-global practical result contained therein can be applied to this problem.

3.2 Inner-loop tracking controller for node $i \in \{1..n\}$

In the inner loop control, a standard linearised quadrotor model at the hovering equilibrium is considered. The equation of motion of the i^{th} quadrotor from (Bouabdallah and Siegwart, 2007) is used here, and is included for completeness as follows:

$$\begin{aligned} \dot{\phi}_i &= p_i; & \dot{p}_i &= \frac{\rho_i^x}{I_x}; & \dot{u}_i &= -g\theta_i + \frac{f^x}{m}; & \dot{x}_i &= u_i \\ \dot{\theta}_i &= q_i; & \dot{q}_i &= \frac{\rho_i^y}{I_y}; & \dot{v}_i &= g\phi_i + \frac{f^y}{m}; & \dot{y}_i &= v_i \\ \dot{\psi}_i &= r_i; & \dot{r}_i &= \frac{\rho_i^z}{I_z}; & \dot{w}_i &= \frac{-f_i^t + f^z}{m}; & \dot{z}_i &= w_i \end{aligned} \quad (4)$$

Here, $(\phi_i, \theta_i, \psi_i)$ are the Euler angles; (p_i, q_i, r_i) and (u_i, v_i, w_i) are angular and linear velocities along quadrotor's body frame x-y-z axis respectively; and (x_i, y_i, z_i) are quadrotor's inertial frame coordinates leading to the overall state vector in the inner loop control $\mathbf{X}_i = [\phi_i, \theta_i, \psi_i, p_i, q_i, r_i, u_i, v_i, w_i, x_i, y_i, z_i]^T \in \mathbb{R}^{12 \times 1}$. The vehicle motors supply thrust force and torques $\mathbf{u}_i^{act} = [f_i^t, \rho_i^x, \rho_i^y, \rho_i^z]^T$, but are potentially corrupted by constant wind disturbances along the inertial frame x-y-z direction $\mathbf{d} = [f^x, f^y, f^z]$.

The inner loop dynamics of (4) can subsequently be written into the compact linearised form

$$\dot{\mathbf{X}}_i = \mathbf{A}\mathbf{X}_i + \mathbf{B}\mathbf{u}_i^{act} + \mathbf{D}\mathbf{d}. \quad (5)$$

The desired height of the UAVs is assumed to be constant at z_i^g , and thus only the (x_i^g, y_i^g) coordinates are required to be specified by the outer (guidance) loop of each agent. An LQR controller is subsequently chosen to regulate \mathbf{X}_i to $\mathbf{X}_i^g = [\mathbf{0}_{9 \times 1}, x_i^g, y_i^g, z_i^g]^T$.

Remark 1. The dynamics of (4) are sufficiently smooth so that Assumption 1 of (Liao et al., 2019) holds.

Remark 2. The formulation of (4) can consider either feedback linearisation or local linearisation approaches. The former leads to the choice of LQR design for the inner loop control ensuring that the linearised dynamics are GAS towards a steady state input-output map, $\mathbf{x} = \mathbf{l}(\mathbf{u})$, and hence Assumption 2 of (Liao et al., 2019) is satisfied - other choices for the inner loop controller that maintain this property are equally valid. However in the latter case with only a locally linear model being considered, only LAS can be concluded and the results of (Liao et al., 2019) collapse to local rather than global conditions.

3.3 Choice of optimisation metric used in guidance loop

For nodes i and j in the chain with their current coordinates on the x-y plane denoted as $\mathbf{x}_i, \mathbf{x}_j \in \mathbb{R}^2$, the transmitted signal power from node j measured by node i is $S(\mathbf{x}_i, \mathbf{x}_j)$. The measured signal power, $S(\mathbf{x}_i, \mathbf{x}_j)$, is utilised to evaluate the communication quality of that link in the chain.

The signal power functions are typically modelled in a Gaussian form, with a potentially temporally- and spatially-varying fading parameter c_{fi} , and a peak power level, K_i , for the i^{th} node given by:

$$S(\mathbf{x}_{i\pm 1}, \mathbf{x}_i) = K_i \cdot \exp(-c_{fi} \|\mathbf{x}_{i\pm 1} - \mathbf{x}_i\|^2) \quad (6)$$

A single (unconstrained) optimisation metric for the entire set of agents would be to improve the bottleneck (or weakest) link by adjusting the reference positions of the agents. In this work, to maintain smoothness in the optimisation metric, the unconstrained problem is posed using the *softmin* function as:

$$h_o(\mathbf{x}) := \Psi\{S(\mathbf{x}_i, \mathbf{x}_j), \forall i, j \in E\} \quad (7)$$

It follows directly from Remark 2 that the following unconstrained optimisation problem for the guidance coordinates can be posed on the steady state manifold:

$$Q(\mathbf{u}) := h_o(\mathbf{l}(\mathbf{u})) = \Psi\{S(\mathbf{u}_i, \mathbf{u}_j), \forall i, j \in E\} \quad (8)$$

$$\mathbf{u}^* := \arg \max Q(\mathbf{u}) \quad (9)$$

Remark 3. It is straightforward to show that the choice of optimisation function (8) is continuously differentiable

everywhere and so satisfies Assumption 3 of (Liao et al., 2019). It is worth noting, however, that in practice the use of dither provides a smoothing effect that mitigates against the need for continuity everywhere in the steady-state map (Zames and Shneydor, 1976). The implication is that $\Psi(\cdot)$ used in (8) can be replaced in practice by a strict *min* operation, potentially simplifying the implementation. Nonetheless, to retain consistency with the developed theory in Liao et al. (2019), the explicit $\Psi(\cdot)$ function is used hereafter in this work.

Remark 4. It is worth noting that the solution to (9) is only approximately equal to the true minimum, however this approximation error can be made arbitrarily small through the choice of c_1 in the definition of $\Psi(\cdot)$. The value of $c = 10$ ensures the approximation error is small in the context of the problems considered in this paper.

As shown in (Dixon and Frew, 2009), under a simple path graph communication topology with fixed end nodes such as considered here, the problem in (9) can be solved distributively by treating $\mathbf{u}_{i\pm 1}$ as constant with respect to the i^{th} node. Thus, given Remarks 2 and 4, the distributed solution to (9) for relay i to solve in the slow time scale can be simplified to:

$$Q_i(\mathbf{u}_i) := \Psi\{S(\mathbf{u}_i, \mathbf{u}_{i+1}), S(\mathbf{u}_i, \mathbf{u}_{i-1})\} \quad (10)$$

$$\mathbf{u}_i^* := \arg \max Q_i(\mathbf{u}_i) \quad (11)$$

3.4 Choice of constraint function

Within the $x - y$ domain we denote the region \mathcal{A} representing the no-fly area in which each of the UAVs cannot remain permanently. Here, the constrained regions are considered to be represented by ellipses, and the (unknown) constraint functions are considered to be quadratic potential functions in a similar methodology to (Zavlanos and Pappas, 2007):

$$G_{\mathcal{A}}(\mathbf{x}) = -\alpha \|\mathbf{x} - \mathbf{x}_{con}\|^2 + K_{con} \quad (12)$$

Here, the parameters $(\mathbf{x}_{con}, K_{con}, \alpha)$ are chosen to ensure that the constraint function has sufficient gradient and satisfies $G_{\mathcal{A}} = 0$ on the boundary of the constraint region, and $G_{\mathcal{A}} < 0$ when the constraint is inactive.

Remark 5. This is clearly a simplistic approximation, although overbounding the disallowed regions with convex polytopes of other shapes is a practical solution. This choice of constraint function ensures that Assumption 4 (convexity of the constraint function) (Liao et al., 2019) is satisfied by design, and furthermore Assumption 5 (a feasible unconstrained solution exists) is satisfied for finite $(\mathbf{x}_{con}, K_{con}, \alpha)$.

3.5 Choice of dither and gradient estimator

The two dither signals in the $x - y$ setpoints for each agent are chosen to be sinusoids of amplitude a , and the gradient estimators in Fig. 2 are chosen to be low pass filters with transfer functions described by $\frac{\omega_i \omega_{Li}}{s + \omega_i \omega_{Li}}$. The outputs of the gradient estimators are denoted $\xi_i := [\xi_i^o, \xi_i^c]^T$.

Remark 6. With this choice of dither and in the case $\omega_i \neq \omega_{i\pm 1}$, it is clear that $\frac{1}{T} \int_0^T \mathbf{r}_i(t) \mathbf{r}_i(t)^T dt =: \mathbf{K} \succ \mathbf{0}$. Hence

it is concluded that Assumption 6 of (Liao et al., 2019), which relates to a persistency of excitation condition, is satisfied.

3.6 Choice of optimiser

As in (Liao et al., 2019), the optimizer \mathbf{F}_γ in the outer-loop combines the objective and constraint function gradients (with the latter weighted by some scaling parameter λ) to generate the guidance setpoint in \mathbb{R}^2 . The optimizer \mathbf{F}_{γ_i} utilises the smooth function (3), and is given by:

$$\mathbf{F}_{\gamma_i}(G_{\mathcal{A}}(\mathbf{x}_i), \begin{bmatrix} \nabla Q_i \\ \nabla G_{\mathcal{A}} \end{bmatrix}) = (1 - \sigma(G_{\mathcal{A}}(\mathbf{x}_i) - \gamma_i)) \nabla Q_i - \sigma(G_{\mathcal{A}}(\mathbf{x}_i) - \gamma_i) \lambda \nabla G_{\mathcal{A}} \quad (13)$$

In (Ramos et al., 2017) dynamics were introduced in the offset parameter, γ_i , to ensure the steady state solution of the extremum seeker is in the feasible constraint set. These dynamics were of the form $\dot{\gamma}_i = -kG_{\mathcal{A}}(\mathbf{x}_i)$ with appropriate antiwindup action added. In this paper, the following smooth antiwindup approach is used which maintains $|\gamma_i| \leq \gamma_{sat}$ by introducing a pseudo-state, g_i , and uses (2):

$$\dot{\gamma}_i = \gamma_{sat} \Omega(g_i) \quad (14)$$

$$\dot{g}_i = \frac{-k\varepsilon\omega_{Li}\omega_i}{\gamma_{sat}} \Omega(G_{\mathcal{A}}(\mathbf{x}_i)) \quad (15)$$

Remark 7. The continuous approximation functions (1)-(3) utilised in (8) - (15) may be replaced by their discontinuous counterparts leading to a hybrid system, which may be dealt with directly as in (Poveda et al., 2018), albeit with assumptions for the closed loop system that are more difficult to satisfy *a priori*.

3.7 Analysis of closed loop system

We can formulate the closed loop equations for the entire closed loop system under a constant disturbance using (4) to (15). For notational convenience, we introduce the variables $\zeta_i := [\Psi(S(\mathbf{u}_i, \mathbf{u}_{i+1}), S(\mathbf{u}_i, \mathbf{u}_{i-1})) \mathbf{r}_i^T, G_{\mathcal{A}}(\mathbf{x}_i) \mathbf{r}_i^T]^T$, and $\mathbf{z}_i := [\gamma_i, g_i]^T$. The overall closed loop system in Fig. 2 can then be represented by the following dynamics:

$$\begin{aligned} \dot{\mathbf{x}}_i &= \mathbf{f}_i(\mathbf{x}_i, \hat{\mathbf{u}}_i + \mathbf{a}\mathbf{r}_i(\omega_i t), \mathbf{d}) \\ \dot{\xi}_i &= -\omega_{Li}\omega_i \cdot (\xi_i - \zeta_i) \\ \dot{\hat{\mathbf{u}}}_i &= \varepsilon\omega_{Li}\omega_i \cdot \mathbf{F}_\gamma\left(G_{\mathcal{A}}(\mathbf{x}_i), \frac{1}{a} \text{diag}(\mathbf{K}^{-1}) \cdot \xi_i\right) \\ \dot{\mathbf{z}}_i &= -\varepsilon\omega_{Li}\omega_i \Omega(G_{\mathcal{A}}(\mathbf{x}_i)) \left[\frac{2ke^{-g_i}}{(1 + e^{-g_i})^2}, \frac{k}{\gamma_{sat}} \right]^T \end{aligned} \quad (16)$$

The desired solution to (16) for the i^{th} relay corresponds to the state $(\mathbf{x}_i^*, \xi_i^*, \mathbf{u}_i^*, \mathbf{z}_i^*)$, which is the steady state solution to the posed constrained optimisation problem, i.e.:

$$\mathbf{u}_i^* := \left\{ \Psi\{S(\mathbf{u}_i, \mathbf{u}_{i+1}), S(\mathbf{u}_i, \mathbf{u}_{i-1})\} \left| G_{\mathcal{A}}(\mathbf{u}_i) \leq 0 \right. \right\} \quad (17)$$

An error system can then be constructed by defining:

$$\begin{aligned} \tilde{\mathbf{u}}_i(t) &= \hat{\mathbf{u}}_i(t) - \mathbf{u}_i^* \\ \tilde{\mathbf{z}}_i(t) &= \mathbf{z}_i(t) - \mathbf{z}_i^* \\ \tilde{\xi}_i(t) &= \xi_i(t) - \xi_i^* \\ \tilde{\mathbf{x}}_i(t) &= \mathbf{x}_i(t) - \mathbf{x}_i^* \end{aligned} \quad (18)$$

The error system dynamics resulting from (16) and (18) are in the same form and all the required Assumptions of Theorem 1 in Liao et al. (2019) hold. Thus, we can conclude that the following SPA result holds for the distributed constrained signal chaining problem:

Corollary 1. Consider (16)-(18), with any positive Δ such that

$$\|\tilde{\mathbf{x}}_i(t_0), \tilde{\xi}_i(t_0), \tilde{\mathbf{u}}_i(t_0), \tilde{\mathbf{z}}_i(t_0)\| \leq \Delta.$$

For any $\nu > 0$, there exists $\beta_1, \beta_2, \beta_3 \in \mathcal{KL}$, such that there exists $(a^*, k^*, \alpha^*) \in \mathbb{R}_{>0}^3$, where for any $(a, k, \alpha) \in (0, a^*] \times (0, k^*] \times \mathbb{R}_{>\alpha^*}$ there exists $\varepsilon^* > 0$, such that for any $\varepsilon \in (0, \varepsilon^*]$ there exists $\omega_L^* > 0$, and for any $\omega_{Li} \in (0, \omega_L^*]$ there exist $\omega_i^* > 0$, such that for any $\omega_i \in (0, \omega_i^*]$ the following holds $\forall t \geq t_0 \geq 0, \forall i = 1..n$:

$$\|\tilde{\mathbf{x}}_i(t)\| \leq \beta_1 \left(\|\tilde{\mathbf{x}}_i(t_0), \tilde{\xi}_i(t_0), \tilde{\mathbf{u}}_i(t_0), \tilde{\mathbf{z}}_i(t_0)\|, (t - t_0) \right) + \nu$$

$$\|\tilde{\xi}_i(t)\| \leq \beta_2 \left(\|\tilde{\xi}_i(t_0), \tilde{\mathbf{u}}_i(t_0), \tilde{\mathbf{z}}_i(t_0)\|, \omega_i \omega_{Li} (t - t_0) \right) + \nu$$

$$\|\tilde{\mathbf{u}}_i(t), \tilde{\mathbf{z}}_i(t)\| \leq \beta_3 \left(\|\tilde{\mathbf{u}}_i(t_0), \tilde{\mathbf{z}}_i(t_0)\|, \omega_i \omega_{Li} \varepsilon k a (t - t_0) \right) + \nu$$

The implication of this result is practical stability for the entire closed loop system operating under a constant disturbance, with tuning guidelines outlined above. In the event that locally linear controllers are used, the result becomes a local result that places an upper bound on Δ .

4. SIMULATION RESULTS

4.1 Distributed algorithm with homogenous agents and no area constraint

To demonstrate the proposed framework, we initially consider the scenario whereby two base stations are positioned at $\mathbf{x}_0 = [0; 0]$ and $\mathbf{x}_{16} = [150; 100]$, and there are no area constraints to contend with. Fifteen identical quadrotors with $m = 0.35\text{kg}$, $I_x = I_y = 8.6 \times 10^{-3} \text{kg m}^2$, $I_z = 2I_x$ are dispatched from a single location $\mathbf{x} = [50, 0]$ to maximise the signal transmission between the bases. The parameters of the agents distributed controllers are shown in Table 1.

The trajectories of the agents upon release are shown in Fig. 3. As might reasonably be expected given the identical nature of the agents and the absence of area constraints, the relays distribute themselves uniformly along the shortest path between the two base stations. This is however an important base case, as it validates that distributing the algorithm in the manner suggested herein does not impact on the ability to achieve the optimum solution.

Table 1. Initial parameters for simulations without area constraints

(K_i, c_{fi}) for (6)	$(2, 0.5 \times 10^{-2})$
$(\varepsilon, \gamma_{sat}, k)$ in (14)-(16)	$(25, 20, 10^{-3})$
Relays $i = 1, 4, 7, 10, 13$	$\mathbf{r} = [\sin(0.02t + \pi/2); \sin(0.02t)];$ $\omega_{Li} = 0.01$
Relays $i = 2, 5, 8, 11, 14$	$\mathbf{r} = [\sin(0.15t); \sin(0.15t + \pi/2)];$ $\omega_{Li} = 0.15$
Relays $i = 3, 6, 9, 12, 15$	$\mathbf{r} = [\sin(0.015t + \pi/2); \sin(0.015t + \pi/7)];$ $\omega_{Li} = 0.014$

This is further illustrated in Fig. 4 where the signal strength across the weakest link in the chain of relays, which is the bottleneck for the overall transmission between the two end nodes, demonstrating that this approaches the global solution.

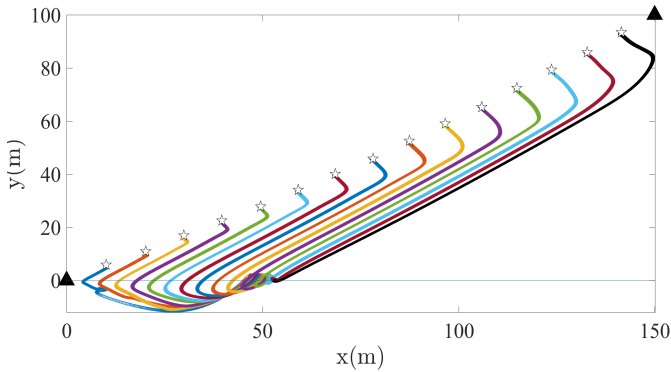


Fig. 3. Trajectories of 15 quadrotor-mounted communication relays (symbol ☆) position evenly between two stations (symbol ▲) at the end of the simulation. All nodes have the same signal power function.

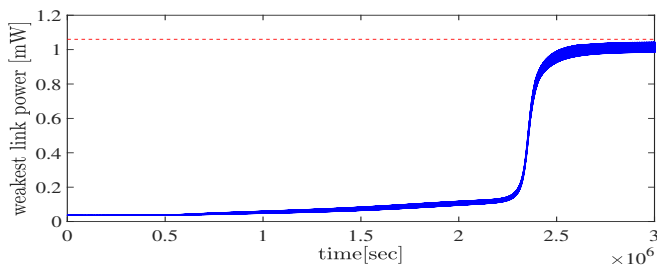


Fig. 4. The team of quadrotors maximise the weakest signal power link within the communication chain. The dash line represents the optimum value.

4.2 Distributed algorithm with homogenous relays and an area constraint

Having established the functionality of the distributed algorithm, area constraints are now imposed that the relays must satisfy in steady state representing a no-fly zone for the UAVs. The no-fly zone is represented by the ellipsoidal potential function centred at (15,15) and described by $G_A(\mathbf{x}) = (-\|\mathbf{x} - [15; 15]\|^2 + 80) \times 10^3$. $G_A(\mathbf{x}) > 0$ is the constrained area, and lies directly in the pathway between the two end points. The number of agents is now reduced to three to allow for clearer illustration, and the base stations are located at $\mathbf{x}_0 = [0; 0]$ and $\mathbf{x}_4 = [25; 25]$. The parameters used in this second simulation are contained in Table 2.

The relays are now released from equally separated positions along the x-axis, and the resulting trajectories are plotted in Fig. 5. This requires two of the relays to transition towards equidistant locations on the boundary of the constrained region, represented by the constrained optima of $\mathbf{x}_1^* = [9.33; 3.72]$ $\mathbf{x}_2^* = [18.87; 7.13]$ $\mathbf{x}_3^* = [23.88; 14.86]$.

As a further test case, force disturbances representing constant wind conditions of positive and negative values are added to the simulation with the results plotted in Fig

Table 2. Parameters for initial simulations with area constraints

(K_i, c_f) for (6)	$(8, 0.5 \times 10^{-2})$
$(\varepsilon, \gamma_{sat}, k)$ in (14)-(16)	$(25, 20, 10^{-3})$
λ in (13)	0.02
Relay 1	$\mathbf{r} = 0.5 \times [\sin(0.01t + \pi/2); \sin(0.01t)];$ $\omega_L = 0.01$
Relay 2	$\mathbf{r} = 0.5 \times [\sin(0.03t); \sin(0.03t + \pi/2)];$ $\omega_L = 0.15$
Relay 3	$\mathbf{r} = 0.5 \times [\sin(0.015t + \pi/2); \sin(0.015t + \pi/7)];$ $\omega_L = 0.014$

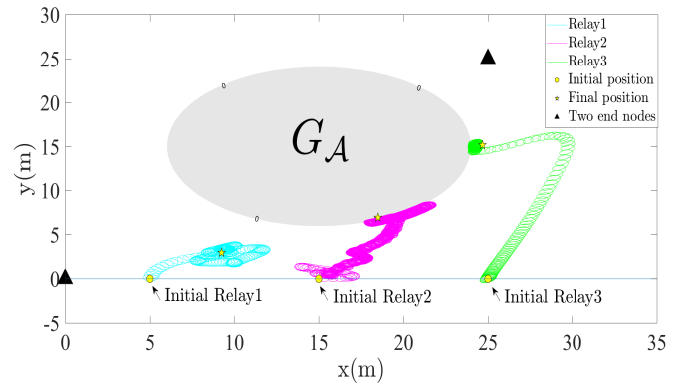


Fig. 5. Stations and relays have the same transmission power function.

6. Despite this causing an offset at the inner loop control, the outer loop simply adjusts the set point to compensate for the impact of these disturbances. Although not plotted, a similar result holds if the constant disturbances differ between agents.

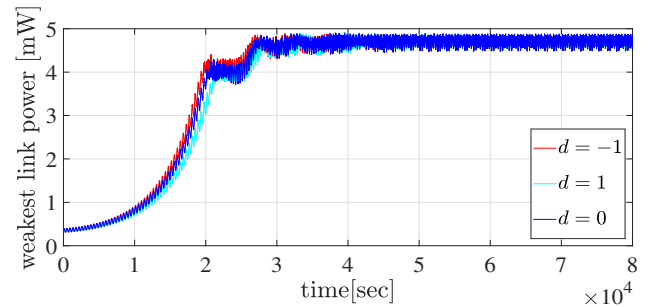


Fig. 6. Bottleneck signal link power under constant force disturbances.

As a demonstration of the impact of tuning parameters on the convergent behaviour, the dither amplitude and optimiser gain are increased to $(a, \varepsilon) = (2.5, 100)$. As expected from Theorem 1 of (Liao et al., 2019) and shown by the offset trajectories relative to these optima in Fig. 7, increasing these gains leads to a faster convergence rate at the expense of larger oscillations around the optima.

4.3 Distributed algorithm with heterogeneous relays and an area constraint

To simulate the effect of heterogeneity amongst the agents, the signal power of the middle relay is now reduced to

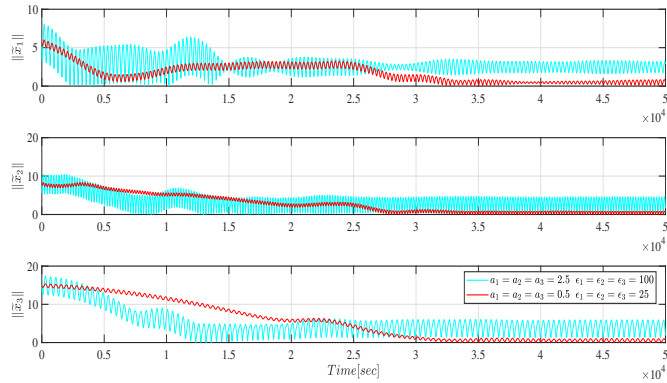


Fig. 7. Position errors $\|\tilde{\mathbf{x}}_1\|$, $\|\tilde{\mathbf{x}}_2\|$, $\|\tilde{\mathbf{x}}_3\|$ of relays using different sets of tuning parameters.

$S(\mathbf{x}_{1,3}, \mathbf{x}_2) = 3 \cdot \exp(\frac{-\|\mathbf{x}_2 - \mathbf{x}_{1,3}\|^2}{2 \cdot 10^2})$. This might represent the battery on this relay is starting to lose power leading to lower available transmission effectiveness. The other relays maintain the same power transmission characteristics as in the earlier simulations. The results demonstrated in Fig. 8 show that the final positions of relays 1 and 3 are closer to the weak relay to compensate for the reduced power. The new constrained optimum obviously has a lower bottleneck link transmission as illustrated in Fig. 9, but roughly the same time to achieve the final positions.

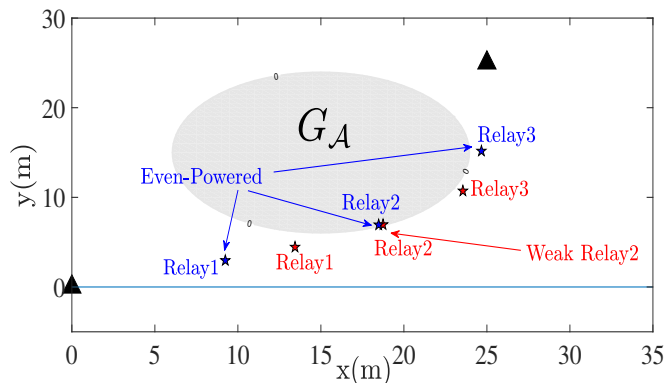


Fig. 8. The middle relay incurs degraded transmission.

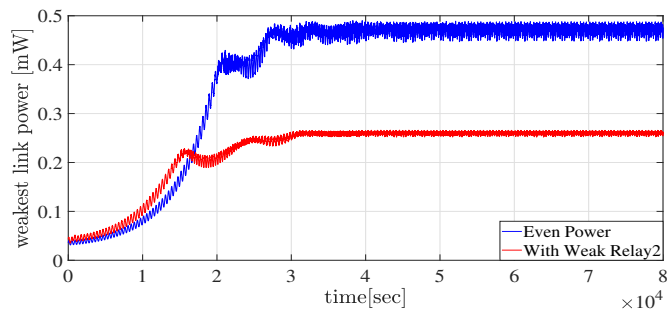


Fig. 9. The bottleneck signal transmission power with homogenous and heterogeneous agents.

5. CONCLUSION

To maximise connectivity across a UAV-based communication network that cannot have agents remain in certain regions, this paper proposes a distributed version of the constrained extremum seeking algorithm presented in Liao

et al. (2019). The considered approach is computationally low, and not impacted by the number of agents in the network. Through a series of simulations the approach is shown to position the UAV-relays to maximise the bottleneck link for signal transmission, leading to positions that obey the area constraints under constant disturbances with both homogeneous and heterogeneous agents.

Further work is required to implement the algorithms on hardware, with further algorithmic refinement to focus on improving the convergence rates through incorporation of known information into the algorithm, and to formally derive conditions under which the end points may be time varying. We will also consider adaptation of the algorithm to account for redundancy requirements, particularly in the face of changes to the underlying graph due to removal of individual agents.

REFERENCES

- Bouabdallah, S. and Siegwart, R. (2007). Full control of a quadrotor. In *2007 IEEE/RSJ International Conference on Intelligent Robots and Systems*, 153–158. IEEE.
- Dixon, C. and Frew, E.W. (2009). Maintaining optimal communication chains in robotic sensor networks using mobility control. *Mobile Networks and Applications*, 14(3), 281–291.
- Dürr, H.B., Stanković, M.S., and Johansson, K.H. (2011). Distributed positioning of autonomous mobile sensors with application to coverage control. In *Proceedings of the 2011 American Control Conf.*, 4822–4827. IEEE.
- Hasan, M.Z., Al-Turjman, F., and Al-Rizzo, H. (2017). Optimized multi-constrained quality-of-service multipath routing approach for multimedia sensor networks. *IEEE Sensors Journal*, 17(7), 2298–2309.
- Liao, C.K., Manzie, C., Chapman, A., and Alpcan, T. (2019). Constrained extremum seeking of a MIMO dynamic system. *Automatica*, 108, 108496.
- Min, B.C., Kim, Y., Lee, S., Jung, J.W., and Matson, E.T. (2016). Finding the optimal location and allocation of relay robots for building a rapid end-to-end wireless communication. *Ad Hoc Networks*, 39, 23–44.
- Poveda, J.I., Kutadinata, R., Manzie, C., Nešić, D., Teel, A.R., and Liao, C. (2018). Hybrid extremum seeking for black-box optimization in hybrid plants: An analytical framework. In *2018 IEEE Conference on Decision and Control (CDC)*, 2235–2240.
- Ramos, M., Manzie, C., and Shehkar, R. (2017). Online optimisation of fuel consumption subject to nox constraints. In *2017 IFAC World Congress*.
- Rawat, P., Singh, K.D., Chaouchi, H., and Bonnin, J.M. (2014). Wireless sensor networks: a survey on recent developments and potential synergies. *The Journal of Supercomputing*, 68(1), 1–48.
- Zames, G. and Shneydor, N. (1976). Dither in nonlinear systems. *IEEE Transactions on Automatic Control*, 21(5), 660–667.
- Zavlanos, M.M. and Pappas, G.J. (2007). Potential fields for maintaining connectivity of mobile networks. *IEEE Transactions on Robotics*, 23(4), 812–816.
- Zhang, C., Siranosian, A., and Krstić, M. (2007). Extremum seeking for moderately unstable systems and for autonomous vehicle target tracking without position measurements. *Automatica*, 43(10), 1832–1839.